Carbohydrate Polymers 95 (2013) 227–232

Contents lists available at SciVerse ScienceDirect

Carbohydrate Polymers

journal homepage: www.elsevier.com/locate/carbpol

Effects of amylose chain length and heat treatment on amylose–glycerol monocaprate complex formation

Xing Zhou[a,b], Ren Wang[b], Yuxian Zhang[b], Sang-Ho Yoo[c], Seung-Taik Lim[a,*]

[a] School of Life Sciences and Biotechnology, Korea University, Seoul 136-701, Republic of Korea
[b] School of Food Science and Technology, Jiangnan University, Wuxi 214122, China
[c] Department of Food Science & Technology and Carbohydrate Bioproduct Research Center, Sejong University, 98 Gunja-Dong, Gwangjin-Gu, Seoul 143-747, Republic of Korea

ARTICLE INFO

Article history:
Received 9 January 2013
Received in revised form 7 February 2013
Accepted 26 February 2013
Available online 5 March 2013

Keywords:
Amylose
Complex
GMC
Heat treatment

ABSTRACT

Aqueous mixtures of amylose with different chain lengths (DP 23–849), which had been enzymatically synthesized or isolated from potato and maize starches, and glycerol monocaprate (GMC, 5:1 weight ratio) were analyzed by using a differential scanning calorimeter (DSC). The mixtures were thermally treated (first DSC scan: 20–140 °C, 5 °C/min and prolonged heat treatment: 100 °C for 24 h) and its effect on the amylose–GMC complex formation was analyzed by DSC and X-ray diffractometer. The amylose, especially short ones, readily associated in the dispersion forming the amylose–amylose crystals but the presence of GMC inhibited the crystal formation. The longer amylose had the greater possibility for the complex formation with GMC, and the prolonged heat treatment facilitated the amylose–GMC complex formation. Both type I and type II complexes were formed during quenching after the initial DSC heating. However, only the type II complexes were formed after the prolonged heat treatment with improved crystallinity and thermostability.

1. Introduction

The linear amylose chains form single helical complexes with a variety of polar lipids usually in crystal states. The amylose–lipid complex formation is of technological importance in food systems, as it reduces stickiness of the starch-based foods, improves freeze–thaw stability, and retards retrogradation of starch. In this way, amylose may have a potential as a carrier for controlled release of various hydrophobic bioactive compounds (Kim & Lim, 2009).

The formation of amylose–lipid complexes is strongly influenced by thermal history. Less ordered complexes (type I) are assumed to be formed at or below 60 °C when a rapid nucleation occurs (Biliaderis & Seneviratne, 1990; Karkalas, Ma, Morrison, & Pethrick, 1995). However, lamellar-like complexes (type II) are formed when the nucleation is slow and propagation is sufficient by elevating temperature (>90 °C) (Biliaderis & Seneviratne, 1990; Gelders, Vanderstukken, Goesaert, & Delcour, 2004).

Complex formation and its crystalline properties are also influenced by the size of aliphatic lipid and amylose chains. Numerous studies have been conducted on the influence of lipid structure on the complex formation with amylose, reporting that the dissociation temperature of amylose–lipid complexes increased with the length of lipid chain (Eliasson & Krog, 1985; Godet, Bizot, et al., 1995; Godet, Tran, et al., 1995; Tufvesson, Wahlgren, & Eliasson, 2003a; Tufvesson, Wahlgren, & Eliasson, 2003b). The effect of amylose chain length has also been studied by several researchers (Gelders et al., 2004; Godet, Bizot, et al., 1995a). However, the amyloses studied were usually obtained by hydrolyzing starch or by isolating amylose from native starches. Those amyloses were either too short (degree of polymerization, DP < 80) or too long (DP ≥ 400). Recently, the amylose with different chain lengths could be synthesized from sucrose using an amylosucrase from *Neisseria polysaccharea* (NpAS). Thus comprehensive investigation on the influence of amylose chain length is possible. In the present study, glycerol monocaprate (GMC) was used as a ligand for the complex formation with amylose with varied chain lengths, and the influence of amylose chain length on the complex formation was investigated. Additionally, the effect of an extensive heat treatment (100 °C for 24 h) for the aqueous mixture of amyloses and GMC was examined.

2. Materials and methods

2.1. Materials

Potato amylose, GMC, and sucrose were purchased from Sigma Chemical Company (St. Louis, MO, USA). *N. polysaccharea* (ATCC 43768) was purchased from the American Type Culture Collection

* Corresponding author. Tel.: +82 2 3290 3435; fax: +82 2 921 0557.
E-mail address: limst@korea.ac.kr (S.-T. Lim).

0144-8617/$ – see front matter © 2013 Elsevier Ltd. All rights reserved.
http://dx.doi.org/10.1016/j.carbpol.2013.02.051

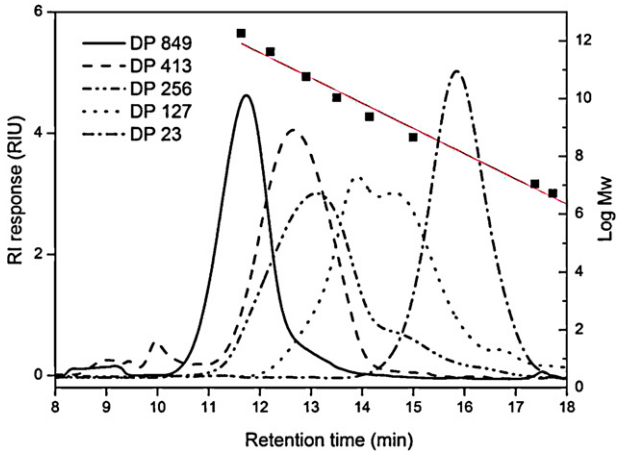

Fig. 1. HPSEC profiles of five amylose with varied chain lengths (DP 23–849) used for complex formation.

(Manassas, VA, USA). Normal maize amylose was isolated from maize starch which was provided by Samyang Genex Company (Seoul, Korea), following the procedure of Jane and Chen (1992). Native normal corn starch was first dispersed in 90% DMSO and precipitate using 95% ethanol. After decanting the supernatant, the precipitate was redissolved in hot water (1.0%, w/v; above 90 °C), and autoclaved at 121 °C for 1 h. The blue screw cap reagent bottle containing the above starch solution was stirred within a boiling water bath for 2 h to completely disperse the starch molecules. n-Butanol (20% by volume) was added, and the solution was stirred at 100 °C for 1 h. The mixture was kept in a Styrofoam box for 24 h at room temperature. The crude amylose–butanol complex was separated by centrifuge (4 °C, 10,000 × *g*, 30 min). Fractionated amylose was further purified by dissolving in DMSO and precipitating using 95% ethanol.

2.2. Amylose synthesis

Recombinant NpAS was cloned and expressed as described previously (Jung et al., 2009). Amylose with varied chain lengths were synthesized by NpAS (400 U/l) from 0.1 M, 0.4 M, and 1.0 M sucrose solutions in 50 mM Tris–HCl buffer solution (pH 7.0) at 35 °C for 18 h (Wang, Kim, Kim, Park, & Yoo, 2011). After the reaction, the mixtures were centrifuged at 5000 × *g* for 10 min, and the precipitate was washed five times with distilled water and then freeze-dried.

The degree of polymerization (DP) of the amylose chains was analyzed by a high-performance size-exclusion chromatography (HPSEC) (Summit HPLC system, Dionex, Sunnyvale, CA, USA) with Shodex OHpak SB-804 and SB-802.5 columns (Showa Denko, Tokyo, Japan) following the procedure of Zhou, Wang, Yoo and Lim (2011). The average DP of each amylose molecule was represented by the apex of the peaks on chromatograms (Fig. 1) which was calculated from the standard curve obtained from glucose, maltotriose, maltopentaose, maltoheptaose and a series of pullulan standards (Showa Denko, Tokyo, Japan) including P5 ($Mw = 5.8 \times 10^3$), P10 ($Mw = 11.8 \times 10^3$), P20 ($Mw = 22.8 \times 10^3$), P50 ($Mw = 47.3 \times 10^3$), P100 ($Mw = 11.2 \times 10^4$) and P200 ($Mw = 21.2 \times 10^4$). AM peak DP was calculated directly from the standard curve. The chain length of amylose could be controlled by using the sucrose solutions of different concentrations: DP 23 from 1.0 M sucrose, DP 127 from 0.4 M sucrose, and DP 256 from 0.1 M sucrose. The maize and potato amyloses used in this study had DP 413, and 849, respectively (Fig. 1).

2.3. DSC sample preparation

GMC (0.4 mg) and amylose (2.0 mg) were dispersed in water (6.0 mg) in an aluminum DSC pan (Seiko Instruments Inc., Chiba, Japan) and hermitically sealed. The control samples were made without GMC or without amylose. These DSC samples were equilibrated at 4 °C for 1 h prior to analysis. To investigate the effect of a prolonged heat treatment, another set of samples were prepared in the same way as mentioned above, and then stored in an oven at 100 °C for 24 h (Tufvesson et al., 2003a). After the prolonged heat treatment, the DSC pans were quench-cooled and then analyzed by DSC.

2.4. DSC analysis

The DSC thermograms were recorded on DSC 6100 (Seiko Instruments Inc., Chiba, Japan). Indium and mercury were used for temperature calibration and an empty pan was used as a reference. All measurements were performed in triplicate. Sample pans were scanned from 20 to 140 °C at a heating rate of 5 °C/min. Samples that were not subjected to a prolonged heat treatment were quench-cooled and immediately rescanned from 20 to 140 °C at a heating rate of 5 °C/min. The melting characteristics of the crystals, including onset (To), peak (Tp), and conclusion (Tc) temperatures, and enthalpy (ΔH) for melting were determined by the EXSTAR6000 Thermal Analysis System (Seiko Instruments Inc., Chiba, Japan).

2.5. X-ray diffraction analysis

GMC (10 mg) and amylose (50 mg) were wetted by 0.5 ml water in an EP tube and stored in an oven at 100 °C for 24 h or heated in an oil bath from 20 °C to 140 °C at a heating rate of 5 °C/min. After the heat treatment, the samples were quench-cooled, dried in a convection oven at 40 °C overnight and ground before analysis. The diffraction patterns were determined by using an X-ray diffractometer (D8 discovery, BRUKER AXS GMBH, Germany), which was operated at 40 mA and 40 kV with the diffraction angles of 3–30° (2θ) and scan speed of 2°/min.

3. Results and discussion

3.1. Thermal transition by initial DSC heating

When an aqueous dispersion of GMC in absence of amylose was heated under a DSC, a sharp GMC melting peak occurred at a temperature around 27 °C with an additional small peak at 92 °C which might be from an impurity (Fig. 2). The control samples containing absolute amylose displayed an endothermic peak for the melting of amylose crystals which was very much different according to the chain length of amylose (Fig. 3A-1). The melting temperature increased but melting enthalpy decreased with the increase in amylose chain length. The smaller amylose chains tended to associate more readily during enzyme synthesis reaction but the resulted crystals melted at lower temperature. However, these synthetic amyloses exhibited typical B-type XRD patterns (indicated by the peak at around 17°) with similar intensities (Fig. 4A). No obvious endothermic peak was observed for the large amylose chains isolated from maize and potato starches (DP 413 and 849). It indicates that the isolation procedure from native starches resulted in the amorphous structure of amylose (Fig. 4A).

Fig. 3A-2 shows the thermograms of the aqueous mixtures of GMC and amyloses (1:5 weight ratio). The large peak around 27.5 °C is responsible for the melting of GMC (Fig. 3A-2). The mixture samples, except that containing potato amylose (DP 849), exhibited thermograms similar to those of pure amylose samples, although the small impurity peak of GMC appeared for all thermograms. The

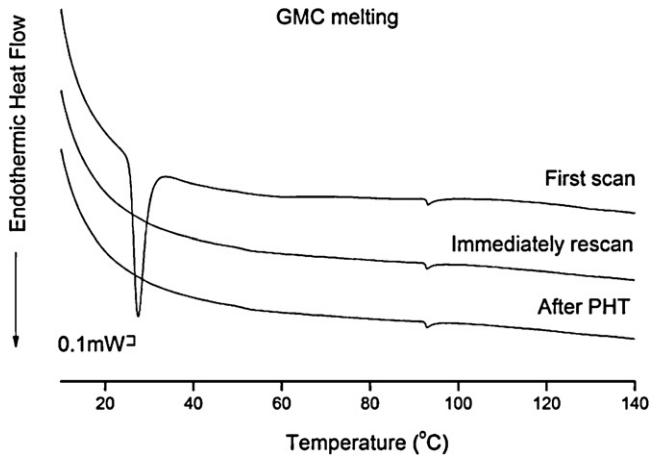

Fig. 2. DSC thermograms of an aqueous GMC dispersion (0.4 mg in 6 mg water) without amylose for the first scan, rescan after quenching, and rescan after a prolonged heat treatment (PHT) (24 h at 100 °C).

melting of amylose crystals occurred in slightly broad ranges, but little affected by the presence of GMC. Only the largest amlyose chain isolated from potato starch displayed a new endotherm at 105–118 °C, which represented a typical melting of amylose–lipid complex (Karkalas et al., 1995). The potato amylose had longest chains and its complex formation with GMC was highly favored. It has been known that the longer the amylose chains are, the greater tendency the complex formation with lipids has (Godet, Bizot, et al., 1995).

3.2. Thermal transition by immediate rescan

The aqueous dispersions of amylose with varied chain lengths were quenched from 140 °C to 20 °C after the initial DSC heating, and then reheated for DSC analysis (rescan). The endotherms for amylose melting were changed by the rescan (Fig. 3B-1). The thermograms indicate that the amylose chains readily recrystallized upon the rapid cooling. However, the newly formed amylose crystals melted at higher temperatures with narrower peaks and slightly smaller enthalpies than those recorded in the first scan. A significant shift of the melting endotherm by near 120 °C was found in the DP 256 amylose crystals. The quench-cooling induced a rearrangement of the amylose crystals improving their thermal stability. As shown in Fig. 4B-1, the recrystallized amyloses still exhibited B-type XRD patterns, but the peaks are sharper which was in agreement with the results obtained by DSC.

The GMC melting peak for recrystallization, which might below 20 °C, was not observed during the rescan after quenching in this experiment (scan from 20 °C to 140 °C), whereas the impurity peak appeared again at the same position (Fig. 2). When the aqueous mixtures of amylose and GMC were rescanned after quenching, the melting peaks of amylose crystals disappeared (Fig. 3B-2). Only the smallest amylose (DP 23) showed a minor peak for its crystal melting at around 80–89 °C, similar to the peak shown without GMC (Fig. 3B-1). This trend revealed that the presence of GMC prevented the recrystallization of amylose. It is widely known that the presence of monoglycerides inhibits starch retrogradation because the monoglycerides tend to form the complex with amylose (Gudmundsson & Eliasson, 1990; Russell, 1987). However, the complex formation between the DP 23 amylose and GMC was not detected on the DSC thermogram. The complex between the amylose and GMC might be less ordered and not in crystalline arrangement. The mixtures containing large amylose chains (DP 256, DP 413, and DP 849) showed a small but new endotherm at 70–80 °C which might represent the melting of amylose–lipid complex. The DP 127 and 256 amylose samples showed an additional small endotherm near the impurity peak at around 95 °C. The amylose chains of DP 413 and 849 exhibited dual endotherms located in relatively high temperature ranges above 100 °C, which

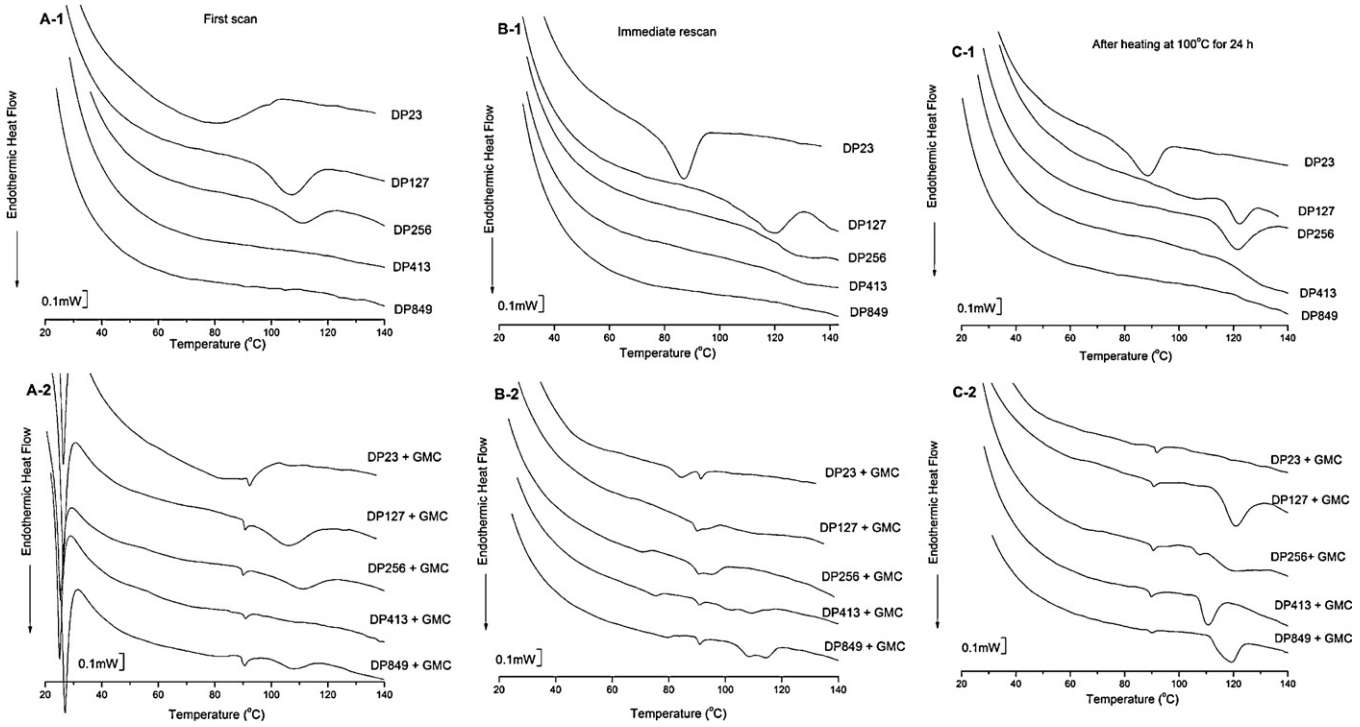

Fig. 3. DSC thermograms of pure amyloses (A-1) and mixtures of amylose and GMC (A-2) for the first DSC scan; DSC thermograms of pure amyloses (B-1) and mixtures of amylose and GMC (B-2) for rescan after quenching; DSC thermograms of pure amylose (C-1) and mixtures of amylose and GMC (C-2) for rescan after a prolonged heat treatment (24 h at 100 °C).

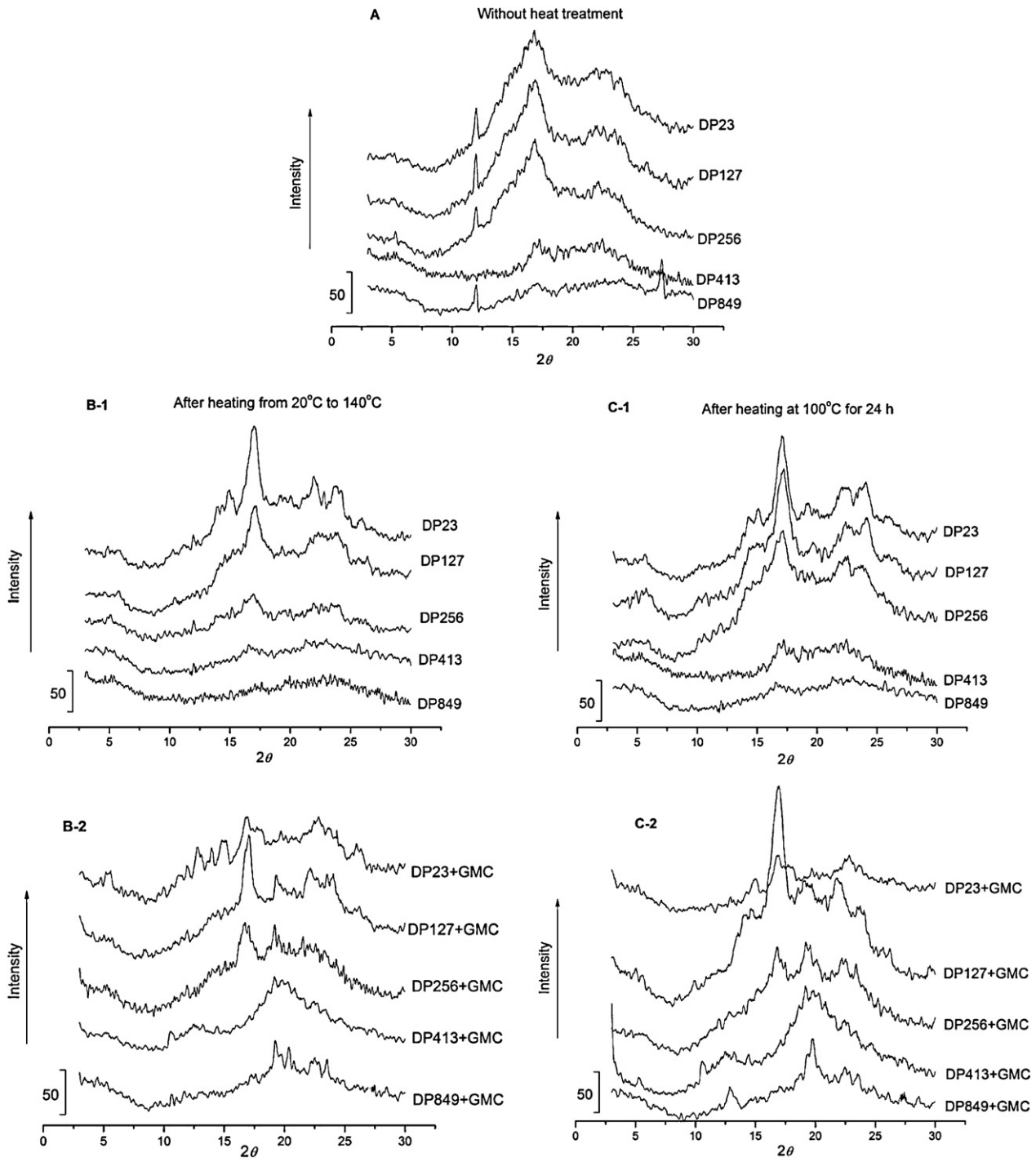

Fig. 4. XRD patterns of pure amyloses without heat-treatment (A); XRD patterns of pure amyloses (B-1) and mixtures of amylose and GMC (B-2) after heating from 20 °C to140 °C; XRD patterns of pure amylose (C-1) and mixtures of amylose and GMC (C-2) after a prolonged heat treatment (24 h at 100 °C).

possibly represented the presence of thermally stable amylose–GMC complexes. The thermograms revealed that the quench-cooling facilitated amylose–lipid complex formation. However, the melting of the complexes induced by the rescan proceeded in multiple transitions, possibly indicating the formation of heterogeneous structures of the complex crystals.

The new melting endotherms located at 70–80 °C with the rescanned mixtures containing the medium and large amylose chains (DP 256, 413, and 849) indicated the presence of type I complexes, whereas the other endotherms appeared at the higher melting temperatures (>95 °C) indicated the presence of type II complexes (Tufvesson & Eliasson, 2000). The type I endotherm moved to a higher temperature range with a larger enthalpy when the amylose chain length increased: from Tp 72.2 °C and ΔH 0.5 J/g for DP 256 to Tp 79.4 °C and ΔH 1.1 J/g for DP 849. The endotherm representing type II complexes also moved to higher temperatures with larger ΔH by increasing the amylose chain length, e.g. from Tp 97.6 °C and ΔH 2.0 J/g for DP 127 to Tp 115.0 °C and ΔH 5.3 J/g for DP 849. Godet, Bizot, et al. (1995) prepared amylose–fatty acid complexes under an optimized condition and found the yield of the complex (the precipitate) increased with an increase in amylose chain length, and that higher DP favored the formation of more

stable complex. Gelders, Goesaert, and Delcour (2005) also found that the longer amylose chains resulted in the formation of the complexes melting at higher temperatures. Likewise the amylose of higher DP formed the GMC complex (type I or type II) of high stability, which melted at higher temperature. The endotherms of the type II complex appeared as double peaks for DP 413 amylose and DP 849 amylose. Karkalas et al. (1995) prepared amylose–stearic acid complexes by heating at 80 °C for different periods, and found that the endotherm presented double peaks when heat was provided for a short period, whereas only a single peak appeared when sufficient heat was provided for 24 h. In this study, the complex was formed just by quenching under a DSC, and thus induced heterogeneous formations of amylose–GMC complexes of different melting characteristics.

The XRD patterns of the mixtures of amylose and GMC after heating from 20 to 140 °C were generally in agreement with the DSC thermal transition properties. As shown in Fig. 4B-2, mixture of DP 23 amylose and GMC exhibited only B-type XRD pattern with a lower intensity than that of DP 23 amylose alone. However, the mixtures containing larger amylose chains (DP 413 and 849) exhibited both B and V-type patterns, indicated by the typical peaks at around 17° and 20°. It might be because the larger sample size was used for the XRD analysis than the DSC analysis, which might resulted in much slower cooling. Therefore, amylose-self recrystallization (B-type XRD pattern) might occur during the cooling stage for the XRD samples.

3.3. Effect of prolonged heat treatment

A prolonged heat treatment was applied to the DSC samples and its effect on the complex formation was examined. The prolonged heat treatment changed the thermal transition behavior of amylose–GMC mixtures (Fig. 3C-2). For the smallest amylose chain (DP 23), the melting endotherm of the amylose crystals formed in absence of GMC was not much different from that recorded by the immediate rescan (Fig. 3B-1 vs. Fig. 3C-1). Because the temperature used for prolonged heat treatment (100 °C) was higher than that for the melting of DP 23 amylose crystals, the amylose remained fully amorphous during the prolonged heat treatment. As shown in the thermograms during immediate rescan (Fig. 3B-1), the amylose chains quickly recrystallized and showed the melting endotherm after first scan in DSC. The medium amylose chain DP 127 exhibited sharper endothermic peak as compared with that in the immediate rescan (Fig. 3C-1 vs. Fig. 3B-1). Because the prolonged heat treatment was done at 100 °C which was near the onset for the crystal melting of amylose, an annealing of amylose chains might occur during the prolonged heat treatment. Due to the annealing, the melting of DP 256 crystals appeared in the larger and sharper endotherm compared to that recorded by the immediate rescan. Accordingly, XRD pattern of the DP 23 amylose after heating at 100 °C for 24 h was similar to that of DP 23 amylose after heating from 20 °C to 140 °C (Fig. 4B-1 Vs. Fig. 4C-1), whereas diffraction peaks of the DP 127 and DP 256 were sharper after prolonged heat treatment because of annealing.

Figs. 3C-2 and 4C-2 show the thermograms and XRD patterns for the mixtures of amylose and GMC after the prolonged heat treatment, respectively. No endothermic peak or notable diffraction peak was found for the smallest amylose (DP 23) whereas the larger amyloses clearly showed melting endotherms and diffraction peaks. The DP 127 and GMC mixture showed a large single endotherm (Tp 118.0 °C) after the prolonged heat treatment, similar to that of the amylose–amylose crystals (Fig. 3C-1 vs. Fig. 3C-2). It was for the melting of the recrystallized amylose, not of the complex, as confirmed by the XRD measurement: DP 127 and GMC mixture showed a B-type pattern (Fig. 4C-2). The inhibition of amylose recrystallization by GMC had been found for the rescanned samples regardless of the amylose chain length (Fig. 3B-2). Despite the inhibition by GMC, the extensive heat treatment was sufficient to induce the recrystallization of the medium amylose chain (DP 127). For the DP 256 mixture sample, however, two peaks (minor peak at Tp 107 °C and major peak at Tp 120 °C) were observed in its thermogram. The major peak might represent the melting of the recrystallized amylose as comparing Fig. 3C-1 and C-2, but the small peak could be from the melting of amylose–GMC complex. As confirmed by the XRD measurement: DP 256 and GMC mixture showed a B and V-type pattern (Fig. 4C-2).

Compared to the immediate rescanning, the prolonged heat treatment (100 °C for 24 h) resulted in the absence of type I endotherm because the treatment temperature was higher than the melting of type I crystals (70–80 °C). The type II endotherms, however, had different melting temperatures depending on the chain length of amylose (approximately 100–120 °C). The largest amylose (DP 849) exhibited the melting endotherm at the highest temperature (Tp 120 °C). The different melting temperatures for the complex melting indicate that the amylose–GMC complexes after the annealing induced by the prolonged heat treatment had different crystalline arrangements depending on the chain morphology of amylose. The X-ray diffraction peaks were sharper and the diffraction intensity around 20°, which indicated the complex formation, was higher for larger amyloses. It was in agreement with the thermal transition properties (Fig. 3C-2 vs. 4C-2). The increased enthalpy (ΔH) for the complex melting and the sharper X-ray diffraction peaks with increased intensity after the prolonged heat treatment clearly revealed that the treatment was effective in the formation of amylose–GMC complex, especially when the amylose chain was large.

4. Conclusions

For the formation of amylose–GMC complex, large amylose chains were more favored than small chains although the formation of amylose crystals was easier with small amylose chains. The GMC presence hindered amylose crystal formation, but caused the complex formation in both type I and type II crystals during quenching after initial DSC heating. A prolonged heat treatment (100 °C for 24 h in this case) provided an annealing effect of type II crystal formation with increased crystallinity and thermostability.

References

Biliaderis, C. G., & Seneviratne, H. D. (1990). On the supermolecular structure and metastability of glycerol monostearate amylose complex. *Carbohydrate Polymers*, *13*(2), 185–206.

Eliasson, A. C., & Krog, N. (1985). Physical-properties of amylose monoglyceride complexes. *Journal of Cereal Science*, *3*(3), 239–248.

Gelders, G. G., Goesaert, H., & Delcour, J. A. (2005). Potato phosphorylase catalyzed synthesis of amylose–lipid complexes. *Biomacromolecules*, *6*(5), 2622–2629.

Gelders, G. G., Vanderstukken, T. C., Goesaert, H., & Delcour, J. A. (2004). Amylose–lipid complexation: A new fractionation method. *Carbohydrate Polymers*, *56*(4), 447–458.

Godet, M. C., Bizot, H., & Buleon, A. (1995). Crystallization of amylose–fatty acid complexes prepared with different amylose chain lengths. *Carbohydrate Polymers*, *27*(1), 47–52.

Godet, M. C., Tran, V., Colonna, P., Buleon, A., & Pezolet, M. (1995). Inclusion exclusion of fatty acids in amylose complexes as a function of the fatty acid chain length. *International Journal of Biological Macromolecules*, *17*(6), 405–408.

Gudmundsson, M., & Eliasson, A. C. (1990). Retrogradation of amylopectin and the effects of amylose and added surfactants emulsifiers. *Carbohydrate Polymers*, *13*(3), 295–315.

Jane, J. L., & Chen, J. F. (1992). Effect of amylose molecular-size and amylopectin branch chain length on paste properies of starch. *Cereal Chemistry*, *69*(1), 60–65.

Jung, J. H., Seo, D. H., Ha, S. J., Song, M. C., Cha, J., Yoo, S. H., et al. (2009). Enzymatic synthesis of salicin glycosides through transglycosylation catalyzed by amylosucrases from *Deinococcus geothermalis* and *Neisseria polysaccharea*. *Carbohydrate Research*, *344*(13), 1612–2161.

Karkalas, J., Ma, S., Morrison, W. R., & Pethrick, R. A. (1995). Some factors determining the thermal-properties of amylose inclusion complexes with fatty-acids. *Carbohydrate Research*, *268*(2), 233–247.

Kim, J. Y., & Lim, S. T. (2009). Preparation of nano-sized starch particles by complex formation with n-butanol. *Carbohydrate Polymers*, *76*(1), 110–116.

Russell, P. L. (1987). The aging of gels from starches of different amylose amylopectin content studied by differential scanning calorimitry. *Journal of Cereal Science*, *6*(2), 147–158.

Tufvesson, F., & Eliasson, A. C. (2000). Formation and crystallization of amylose–monoglyceride complex in a starch matrix. *Carbohydrate Polymers*, *43*(4), 359–365.

Tufvesson, F., Wahlgren, M., & Eliasson, A. C. (2003a). Formation of amylose–lipid complexes and effects of temperature treatment. Part 1. Monoglycerides. *Starch-Starke*, *55*(2), 61–71.

Tufvesson, F., Wahlgren, M., & Eliasson, A. C. (2003b). Formation of amylose–lipid complexes and effects of temperature treatment. Part 2. Fatty acids. *Starch-Starke*, *55*(3–4), 138–149.

Wang, R., Kim, J.-H., Kim, B.-S., Park, C.-S., & Yoo, S.-H. (2011). Preparation and characterization of non-covalently immobilized amylosucrase using a pH-dependent autoprecipitating carrier. *Bioresource Technology*, *102*(10), 6370–6374.

Zhou, X., Wang, R., Yoo, S.-H., & Lim, S.-T. (2011). Water effect on the interaction between amylose and amylopectin during retrogradation. *Carbohydrate Polymers*, *86*(4), 1671–1674.